Reproductive Toxicology 102 (2021) 43–55

Contents lists available at ScienceDirect

Reproductive Toxicology

journal homepage: www.elsevier.com/locate/reprotox

The brominated flame retardants TBECH and DPTE alter prostate growth, histology and gene expression patterns in the mouse

Ceyhun Bereketoglu [a,1], Carina Modig [a], Ajay Pradhan [a], Patrik L. Andersson [b], Sotiria Stasinopoulou [c], Dimitra J. Mitsiou [c], Michael N. Alexis [c], Per-Erik Olsson [a,*]

[a] Biology, The Life Science Center, School of Science and Technology, Örebro University, SE-701 82, Örebro, Sweden
[b] Department of Chemistry, Umeå University, SE-901 87, Umeå, Sweden
[c] Molecular Endocrinology Program, Institute of Chemical Biology, National Hellenic Research Foundation, Athens, Greece

ARTICLE INFO

Keywords:
TBECH
DPTE
Prostate
Androgenic
Anti-androgenic
Gene expression

ABSTRACT

The brominated flame retardants (BFRs), 1,2-dibromo-4-(1,2 dibromoethyl)cyclohexane (TBECH) and 2,3-dibromopropyl-2,4,6-tribromophenyl ether (DPTE) bind to the androgen receptor (AR). *in vitro* bioassays have shown that TBECH is a potent androgen agonist while DPTE is a potent AR antagonist. Both TBECH and DPTE alter gene expression associated with AR regulation. However, it remains to be determined if TBECH and DPTE can affect the prostate. For this reason, we exposed CD1 mice to a 1:1 mixture of TBECH diastereomers α and β, a 1:1 mixture of γ and δ, and to DPTE, and tested their effects on prostate growth, histology and gene expression profiles. Castrated mice were used to study the androgenic effects of TBECHαβ and TBECHγδ while the antagonistic effects of DPTE were studied in non-castrated mice. We observed that testosterone and TBECHγδ increased body and prostate weights while TBECHαβ affected neither of them; and that DPTE had no effect on body weight but reduced prostate weight drastically. Histomorphometric analysis of the prostate revealed epithelial and glandular alterations in the TBECHγδ group comparable to those in testosterone group while alterations in the TBECHαβ group were less pronounced. DPTE displayed androgen antagonist activity reminiscent of castration. The transcription profile of the prostate was altered by castration and exposure to testosterone and to TBECHγδ reversed several of these changes. Testosterone and TBECHγδ also regulated the expression of several androgen responsive genes implicated in prostate growth and cancer. While DPTE resulted in a drastic reduction in prostate weight, it only affected a small number of genes. The results indicate that TBECHγδ and DPTE are of high human health concern as they may contribute to changes in prostate growth, histology and function.

1. Introduction

Androgens are required for growth, development, and proper prostate function [1,2]. Androgens function by binding and activating the androgen receptor (AR), which then regulates gene transcription [3,4]. Altered AR activity can result in abnormal prostate development [2,4]. Anthropogenic compounds that act as AR agonists or antagonists may disrupt the endocrine system by interfering with the biological activity of sex hormones and are of great concern for their possible effects on human health [5].

Brominated flame retardants (BFRs) are widely used in commercial and industrial products to reduce their flammability [6,7]. The use of BFRs increased from 145,000 tons in 1990 to 310,000 tons in 2000 worldwide, and reached 465,000 tons in Europe alone in 2006, resulting in increased levels in the environment [6–8]. Due to their toxic effects on the endocrine, metabolic, neurological and reproductive pathways [9–11], several BFRs have been banned and new BFRs have been introduced as replacements.

An emerging BFR, 1,2-Dibromo-4-(1,2dibromoethyl)cyclohexane (TBECH) is produced as a 1:1 mixture of TBECH αβ under the trade name Saytex BCL-462 (Albermarle Corporation, Baton Rouge, LA, USA). TBECH was first detected in 1996 in sediments near a plastics plant in Haifa, Israel [12]. TBECH has since been detected in indoor air at concentrations up to 440 pg/m^3 and in dust up to 130 pg/m^3, in the food

* Corresponding author.
E-mail address: per-erik.olsson@oru.se (P.-E. Olsson).
[1] Present address: Iskenderun Technical University, Faculty of Engineering and Natural Sciences, Department of Biomedical Engineering, Hatay, Turkey.

https://doi.org/10.1016/j.reprotox.2021.04.002
Received 18 December 2020; Received in revised form 22 March 2021; Accepted 7 April 2021
Available online 10 April 2021

web of internal waters and marine waters, in marine mammals, in human breast milk and in serum of school children in China, thus posing a potential threat to humans [13–20]. Although the exact amount of usage is difficult to obtain, the annual production volume of TBECH in the U.S. was estimated to be in the range of 226 tons per year in 2002 [21,22]. The presence of 4 chiral carbons in TBECH results in four diastereomers, α, β, γ, and δ, each of which has its own pair of enantiomers. Technical mixtures of TBECH contain equimolar amounts of the α and β diastereomers, which are thermally converted to the γ and δ diastereomers at temperatures above 123 °C [23].

Using *in vitro* studies, we identified TBECH as an androgen agonist in humans, chicken and zebrafish [24–27]. While TBECHγ and TBECHδ are equally potent as dihydrotestosterone (DHT) in activation of human AR, TBECHα and TBECHβ are partial AR agonists [25,26]. Exposure to TBECH results in upregulation of several AR responsive genes including the induction of prostate specific antigen (PSA), a biomarker for prostate cancer (PCa) [25].

Another BFR, 2,3-dibromopropyl-2,4,6-tribromophenyl ether (DPTE), first reported in 1929 [28], was produced and distributed under the trademark Bromkal 73-5 PE by Chemische Fabrik Kalk until a fire incidence in a factory in 1985. Later, the production of DPTE was stopped and its distribution remains unknown [29]. Reported concentrations of DPTE are up to 1940 μg/kg dry weight (dw) in sewer slime [30] and 1200 μg/kg in household dust [31]. We recently identified DPTE as an androgen antagonist that downregulates AR and androgen response genes in humans, chicken and zebrafish cell lines [32–34].

Besides affecting AR regulation, TBECH also alters thyroid hormone and sex hormone levels in rats, birds and fish [35–37]. TBECH diastereomers also interfere with reproductive functions in animals [38, 39]. DPTE on the other hand is shown to be antiandrogenic, detected in the marine food web and in food markets in China, and frequently detected in animals and humans [29,40–43]. However, the effects of DPTE on reproductive functions remain to be determined. The prostate is an important organ for reproduction and is sensitive to endocrine disrupting compounds [44]. We, therefore, analyzed the effects of TBECH and DPTE on mouse prostate growth, histology and gene regulation. We also evaluated the androgen-regulated gene networks in response to these compounds to obtain a better understanding of the possible effects of BFRs on prostate development.

2. Materials and methods

2.1. Compounds and chemicals

As the individual TBECH diastereomers were not available and as the commercial mixture is a 1:1 mixture of TBECHαβ we used a 1:1 mixture of TBECHαβ in the present study. We also used a 1:1 mixture of the TBECH diastereomers that are formed following a fire, TBECHγδ. TBECH, DPTE, allyl 2,4,6-tribromophenyl ether (ATE), and 2-bromoallyl 2,4,6-tribromophenyl ether (BATE) were synthesized at 98 % purity by Wellington Laboratories (Guelph, Canada) whereas testosterone enanthate (TE), 2,2′,4,4′-Tetrabromodiphenyl ether (BDE-47) and 2,2′,4,4′,5-pentabromodiphenyl ether (BDE-99) were purchased from Sigma Aldrich (USA). The inclusion of ATE, BATE, BDE-47 and BDE-99 in the study was made to compare the tissue distribution of TBECH and DPTE to these substances.

For chemical analysis, the analytical standard for ATE was obtained from AccuStandard (New Haven, CT, USA). BATE, BDE-47 and BDE-99 standards were obtained from Cambridge Isotope Laboratories (Andover, MA, USA). DPTE was obtained from Wellington Laboratories (Guelph, ON, Canada) and TBECH from Wellington Laboratories (Guelph, ON, Canada) and Sigma-Aldrich (now Merck KGaA, Darmstadt, Germany). Stock solutions of chemicals were prepared in toluene. Labeled (13C) internal standards (BDE-47 and BDE-99) were bought from Cambridge Isotope Laboratories (Tewksbury, MA, USA). The labeled compounds were used as internal standards and were added to the samples before extraction, to correct for losses during the clean-up procedure. In the quantification procedure 13C-labeled BDE-47 was used as an internal standard for ATE, BATE, DPTE and TBECH, and 13C-labeled BDE-99 for the native BDE-99. Labeled (13C) PCB 208 was used as a recovery standard (added to samples prior to injection) and was bought from Wellington Laboratories (Guelph, ON, Canada).

Acetone, n-hexane, dichloromethane and toluene (all SupraSolv) were bought from Merck KGaA (Darmstadt, Germany). Diethyl ether (GPR Rectapur) was bought from VWR International (Stockholm, Sweden) and tetradecane from Sigma-Aldrich, now Merck (Darmstadt, Germany).

2.2. Animals and treatments

The experiments were carried out using 42-day old male CD1 mice purchased from Charles River (*via* Indipendenza, 11 - 23885 Calco LC – Italy). Animal handling and experimental procedures were carried out in a certified animal facility (certification no: EL 25 BIO 031-033; approval for animal experiment: No 715488/11.11.2019) under full veterinary monitoring in accordance with EU Directive 2010/63/EU on the protection of animals used for scientific purposes. A licensed experimental protocol (license number 82830-30) was used as follows. Mice were treated humanely to alleviate distress and discomfort and the experimental protocol was approved by the Institutional Animal Care Committee of the National Hellenic Research Foundation. Mice were kept at 22 ± 2 °C, 55–60 % humidity, under a constant photoperiodic cycle (12 h light:12 h darkness) and with free access to standard pelleted rodent diet and sterilized tap water. Thirty-six mice were orchiectomized under anesthesia by intraperitoneal injection of 10 mg ketamine/kg body weight (bw) and 50 mg valium/kg bw. Analgesia during the 1-week recovery period was achieved by intraperitoneal injection of carprofen (20 mg/kg bw/day). Seven days after orchiectomy, castrated (C) mice were allocated randomly into four groups of 9 animals and similar initial BW and BW average in each group, and received daily, for 9 consecutive days, a subcutaneous injection of TBECHαβ (1 mg/Kg bw/day), TBECHγδ (1 mg/Kg bw/day), TE (0.4 mg/Kg bw/day; Sigma-Aldrich) or vehicle (corn oil containing 10 % DMSO). Similarly, non-castrated (NC) mice were distributed randomly into two groups of 9 animals each and received daily for 9 consecutive days a subcutaneous injection of DPTE (1 mg/Kg bw/day) or the above vehicle. All injected compounds were dissolved in DMSO and diluted with 9 volumes of corn oil to a final concentration of 10 mg/mL. Dosing of mice was based on BW as assessed daily and dose volumes did not exceed 0.5 μl/g of BW. A schematic representation of the procedure is shown in Fig. S1. The BWs of the mice were recorded daily. Mice were sacrificed by cervical dislocation at day 10, whole prostate tissue from six mice was collected, snap-frozen in liquid nitrogen, and stored in liquid nitrogen for RNA extraction, while whole prostate tissue from three mice was fixed in formalin for 24 h and embedded in paraffin for histopathological examination. In the light of the principle of 3Rs for the welfare of animals [45], which asks for animal numbers used in research to be reduced as much as possible, the prostates of three castrated animals were used for histopathological examination, given that three biological replicates is the minimum for any statistical analysis, and the prostates of the remaining six castrated animals were amassed in one group used for RNA isolation, since castration-induced prostate involution results in a tiny mass available for mRNA isolation. To determine the tissue distribution of the tested compounds, 6 intact mice were injected with a mixture of DPTE, TBECH (equal amounts of TBECHαβ and TBECHγδ), ATE, BATE, BDE-47, and BDE-99 (1 mg/Kg bw/day), for 6 consecutive days. On day 7, mice were sacrificed by cervical dislocation followed by decapitation. Trunk blood, prostate, liver, fat, testis and brain samples were collected and circulating and tissue levels of each of the compounds were determined. All the determinations were performed in triplicates.

2.3. Sample preparation for compound distribution analysis

All tissue samples were stored in liquid nitrogen before pretreatment and extraction, and all glassware was heated at 550 °C and washed with pure organic solvents before use. The samples were homogenized with dried Na2SO4 using a mortar until a powdery consistency was achieved. Extractions were performed in open columns using two solvents mixes; acetone and n-hexane (5:2) then n-hexane and diethyl ether (9:1). The extracts were enriched with internal standards and cleaned-up on a multi-layer silica column packed with glass wool, KOH-silica, neutral silica, 40 % (w/w) H2SO4 silica, and Na2SO4, pre-rinsed with solvent and eluted with a mixture of n-hexane and dichloromethane (1:1). Finally, prior to GC–MS analysis a recovery standard (13C-labeled PCB 208) was added to the extracts.

2.4. GC–MS analysis

The analytes were quantified using Single Ion Monitoring (SIM) mode by gas chromatography (GC)–high-resolution mass spectrometry (HRMS) with a resolution (at 10 % valley) of about 10000 using an Agilent 6890 gas chromatograph (Agilent Tech., Santa Clara, CA, USA) coupled to an Autospec Ultima mass spectrometer (Waters Corp., Milford, MA, USA). The samples were injected using splitless mode and the compounds separated on a 60 m × 0.25 mm id, DB5-MS column (0.25 μm film, Agilent J&W, Santa Clara, CA, USA). The oven temperature was initially held at 180 °C for 2 min then increased by 5 °C per min to 260 °C, then increased by 10 °C–325 °C and held constant for 8 min. The HRMS was operated with electron impact ionization with electron energy of 35 eV and the ion source temperature was set at 250 °C. Due to limits in the detection system TBECH is reported as a sum of all diastereomers.

2.5. Quality assurance

Laboratory blanks were analyzed in parallel to the samples to ensure that contamination during homogenization, clean-up and instrumental analysis did not significantly influence the results. No BFRs were found in the laboratory blanks. A BFR was considered detected if its signal-to-noise ratio was >3. The limit of detection (LOD) was based on the signal-to-noise in the quantification standard. The average recoveries of the internal standards 13C-labeled BDE-47 and BDE-99 were 81 % and 74 %, respectively. The levels given for BFRs were not calculated using corresponding labeled standards.

2.6. Histopathological analysis

Prostates were fixed in 10 % neutral-buffered formalin (Atom Scientific) and embedded in paraffin. Paraffin sections (4 μm) were cut using a Thermo Scientific Shandon finesse E + microtome. Sections were stained with hematoxylin (Harris Acidified)/ eosin (Atom Scientific 1%), using a Thermo Scientific Gemini AS H&E slide stainer. Microscope slides were examined, and images were taken by standard light microscopy using a Leica DM750 microscope and a Leica ICC50W camera respectively.

2.7. RNA extraction and microarray analysis

Total RNA was extracted from liquid nitrogen-frozen tissue following the enzymatic lysis protocol provided with the RNeasy Mini Kit (Qiagen, Venlo, Netherlands). The quantity and quality of the RNA samples were analyzed with a NanoDrop ND-100 UV–vis spectrophotometer (Thermo Fisher Scientific Inc., Waltham, MA, USA). RNA integrity (RIN) was estimated using an Agilent Bioanalyzer 2100 (Agilent Technologies, Santa Clara, CA, USA) device with an RNA 6000 Nano Assay kit (Agilent Technologies). The samples with RIN values of 7–10 were used for further analysis. Microarray analysis was performed on Cambridge Genomic Services (Department of Pathology, Cambridge University, Cambridge, UK) using Illumina Bead Station 500 according to manufacturer's instructions. Preprocessing of the raw microarray data (presented as. txt files) was performed using Partek Genomics Suite 6.6 (Partek Incorporated, Missouri, USA). Data were normalized and an FDR corrected p value of $p < 0.05$ was used to identify significantly differentially expressed genes (DEGs). The regulated genes were then used for gene set enrichment analysis (GSEA) based on Gene Ontology (GO) annotations. GO enrichment analyses were performed with a p value threshold of 0.05 on Partek Genomics Suite 6.6 and overrepresented GO biological process terms were determined. To find significantly enriched pathways, functional annotation analyses were conducted using the DAVID Bioinformatics Database (https://david.ncifcrf.gov/home.jsp). Common genes were identified by comparing data from different conditions and presented as a Venn diagram.

2.8. Quantitative real-time PCR (qRT-PCR) validation

Equivalent amounts of the total RNA were converted to cDNA using qScript cDNA synthesis kit (Quanta Biosciences, USA) according to the manufacturer's instructions. qRT-PCR was performed on a CFX96 Real-Time PCR Detection System using SsoAdvanced SYBR Green (BioRad, USA). Thermocycling conditions for SYBR Green comprised a denaturation step at 95 ºC for 5 min, followed by 40 cycles at 95 ºC for 2 s and 60 ºC for 30 s. The primers used for the analyses were either obtained from PrimerBank (https://pga.mgh.harvard.edu/primerbank/) or designed using Primer-BLAST, (NCBI-NIH, https://www.ncbi.nlm.nih.gov/tools/primer-blast/) and are presented in Table S1. The comparative Ct method was used to calculate the relative gene expression using the formula 2(-ΔΔCt) for gene expression patterns and the formula 2(-ΔCt) for ratios of gene expression (85). Beta actin (Actb) was used as a normalizing control to analyze gene expression. This gene was chosen because there was no change in the mRNA expression in our microarray data.

2.9. Statistical analysis

All the statistical analysis was performed using the Graphpad Prism software, version 8 (GraphPad, USA) and one-way ANOVA with Dunnett's multiple comparison test. To quantify histological changes, Welch's *t*-test was used.

3. Results

3.1. Tissue distribution

To determine TBECH and DPTE organ distribution in relationship to other chemicals, a mixture of ATE, BATE, BDE-47, BDE-99, TBECH and DPTE was injected subcutaneously into mice and the levels were analyzed in prostate, liver, fat, testis, brain and blood of mice (Table 1). The level of DPTE and BDE-47 exceeded that of the other compounds and was highest in fat, followed by prostate, liver, testis, brain and blood. The distribution of all six compounds across the 6 tissues showed similar patterns. Interestingly, the level of DPTE was ~10-fold higher than TBECH in the prostate. Due to the unavailability of detection system for individual TBECH diastereomers, we report the total TBECH concentrations.

3.2. Body weight and prostate weight

We determined the effects on BW and prostate weight (PW) following separate injections of DPTE, TBECHαβ, TBECHγδ and TE (Fig. 1). Both TE and TBECHγδ injections resulted in a small but significant increase in BW (9.0 and 8.1 % respectively). As the mice grew during the experiment the PW was determined as percentage of the BW. In the NC mice the PW was 6.25 % of the BW. Following castration, the

Table 1
Compound distribution in tissues. Mice received daily injections of mixture for 6 days. On day 7 the mice were sacrificed; selected tissue samples were collected, and compound concentrations were measured and expressed as ng of compound per g of fresh tissue. The data (n = 3) is presented as mean ± standard error of the mean (SEM).

Compound	Fat	Prostate	Liver	Testis	Brain	Blood
ATE	173 ± 18	50 ± 15	20 ± 6	7.0 ± 1.0	0.57 ± 0.21	<0.1
BATE	305 ± 27	81 ± 25	20 ± 7	11 ± 1	0.60 ± 0.07	<0.1
DPTE	4162 ± 308	842 ± 226	221 ± 87	78 ± 12	4.8 ± 0.01	<1
TBECH	473 ± 46	39 ± 12	7.2 ± 2.3	5.2 ± 0.1	0.43 ± 0.05	0.10 ± 0.01
BDE#47	1751 ± 70	489 ± 143	177 ± 51	73 ± 13	8.2 ± 1.0	0.77 ± 0.29
BDE#99	2.17 ± 0.19	0.92 ± 0.17	0.35 ± 0.16	0.15 ± 0.01	0.04 ± 0.02	0.03 ± 0.01

PW was drastically reduced to 2.04 % of the BW. Injection of TE in C mice abrogated the effect of castration (PW 5.74 % of the BW) while injection of TBECHγδ resulted in a small but significant increase in PW to 3.25 % of the BW. Injection of DPTE into NC mice mimicked the effect of castration as the PW was reduced to 2.45 % of the BW.

3.3. Histopathological analysis

To determine if the different treatments resulted in physiological alterations of the prostate, we performed histopathological analysis on prostate tissue following castration and treatments with TBECH, DPTE and TE. We stained prostate sections and examined three of its compartments: ventral prostate (VP), dorsolateral prostate (DLP), and anterior prostate (AP). The histology results revealed that the main architectural and epithelial alterations in the different treatment groups were observed in VP and DLP, while AP did not show any significant change among the groups.

More specifically, in the NC mice, VP and DLP showed moderate to large acini lined by mainly cuboidal to low columnar epithelium with only focal minimal epithelial tufting and infoldings (Figs. 2A, 3 A and 4 A). In the C mice, the VP and DLP appeared to be atrophic compared to the NC mice with a significant decrease in the number and size of the acini (Figs. 2B and S2). Furthermore, in the C mice, adipose tissue was observed in the stroma, while the lining epithelium was low to tall columnar, with minor tufting (Figs. 3B, 4 B and S2). Meanwhile, low mitotic activity was observed in the NC mice, while no mitotic activity was observed in the other groups of animals (Figs. 3A and 4 A).

In the TE-treated mice, VPs showed a significant increase in the total number of acini compared to the C and NC mice. In both the VP and DLP, the mean diameter of the acini was significantly larger than in the C mice and similar to that of the NC mice (Fig. S2). Prominent tufting and focal papillary formations were also observed particularly at the peripheral (*i.e.* distal from the urethra) region of the VP and DLP (Figs. 3C and 4 C) [46,47].

In the TBECHαβ-treated mice, prominent adipose tissue was observed within the stroma (Fig. 2D). The number of acini in the VP was significantly reduced compared to the NC and TE mice, while the acini diameter in the DLP was significantly larger than in the C mice and comparable to TE mice. The lining epithelium was columnar with less tufting and infoldings compared to the NC and TE mice and with

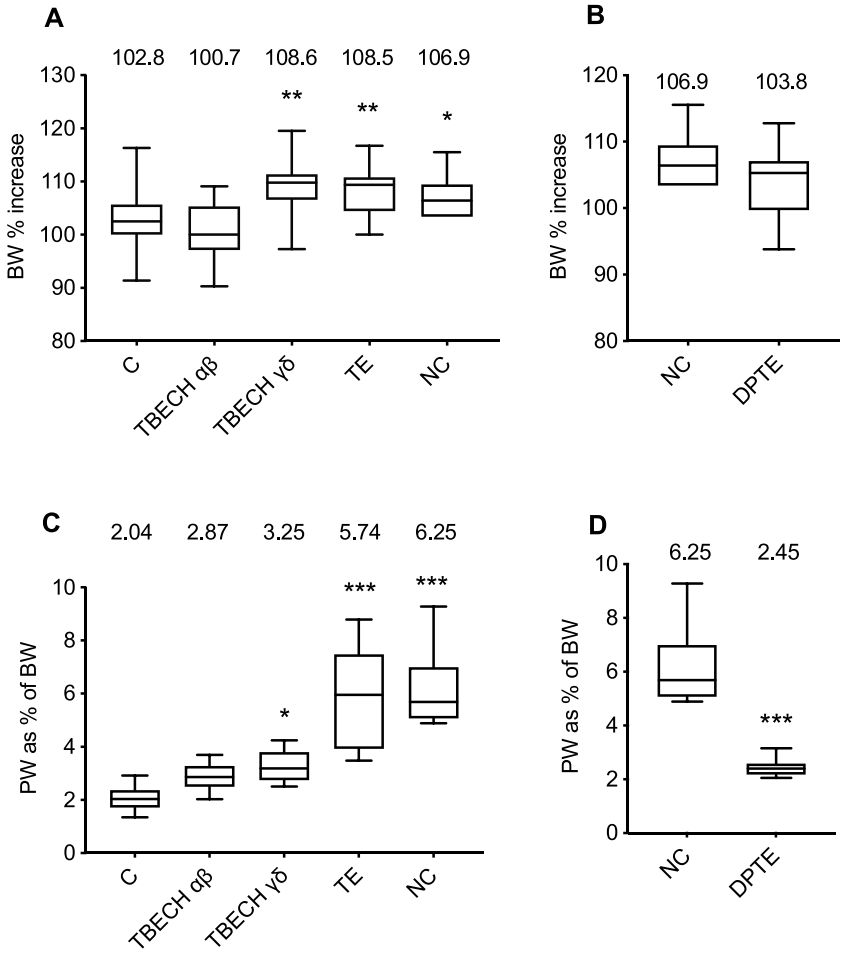

Fig. 1. Body and prostate weight change during the exposure period.
TBECHαβ, TBECHγδ, TE- and vehicle-injected castrated (C) mice were weighed before and after the 10 days exposure (A). Body weight (BW) before injection was set at 100 %. Body weight increase of non-castrated mice (NC) injected with vehicle- or DPTE (B). After exposure, the prostate was weighed (PW) and related to body weight (C and D). Statistical significance was tested using one-way ANOVA with Dunnett's multiple comparison test.

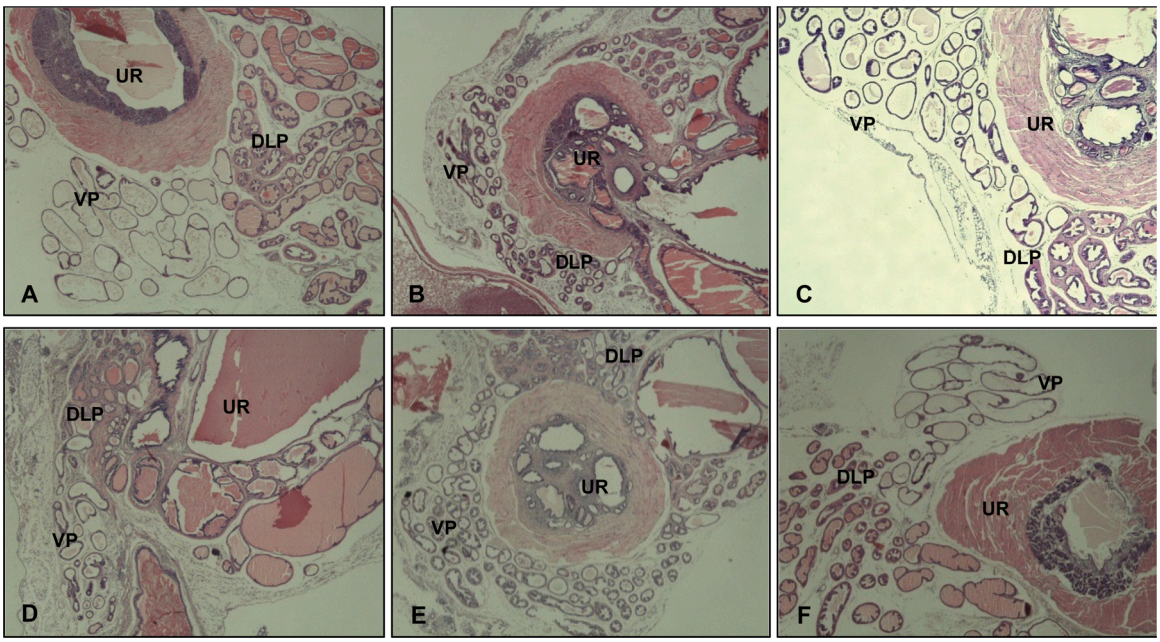

Fig. 2. Change of histological characteristics of ventral and dorsolateral prostate; low magnification. (A) Ventral prostate (VP) and Dorsolateral prostate (DLP) (×20) for non-castrated (NC) mice: no areas of hyperplasia or atrophy. (B) VP and DLP (×20) for C mice: reduction in the number and size of acini; adipose tissue in the stroma. (C) VP and DLP (×20) for TE mice: hyperplasia, with increase in the number of acini (compared to NC and C mice). (D) VP and DLP (×20) for TBECHαβ mice: reduction of the number of acini (compared to NC and C mice), most prominent in VP, and adipose tissue in the stroma. (E) VP and DLP (×20) for TBECHγδ mice: increase in number of acini especially in the VP (compared to NC mice). (F) VP and DLP (×20) for DPTE mice: reduced number of acini compared to NC mice.

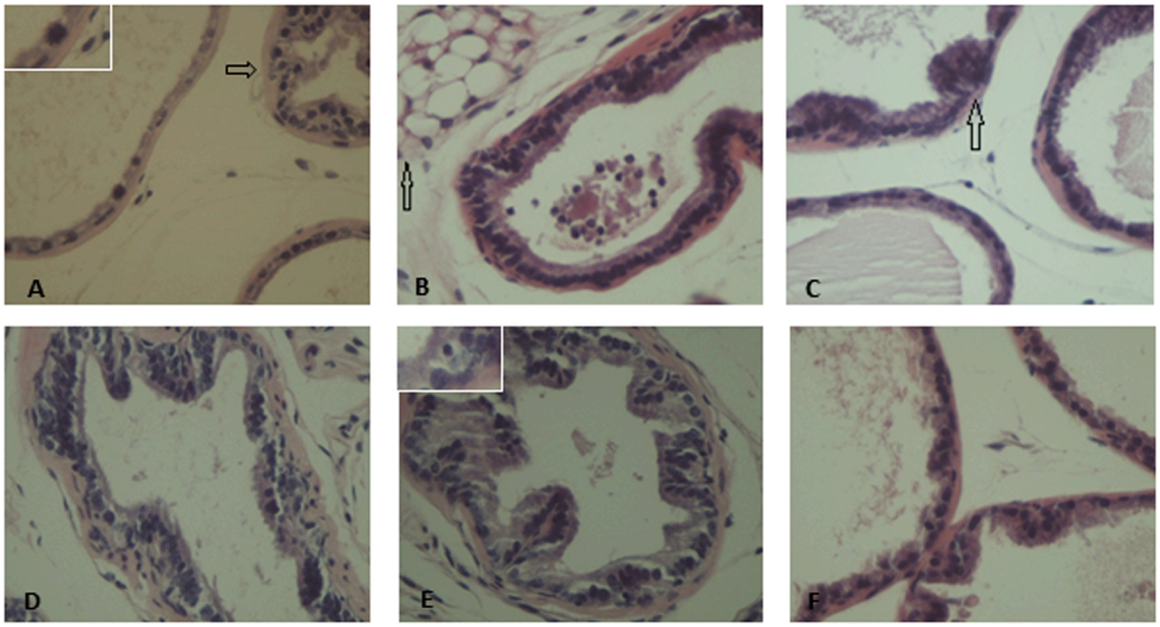

Fig. 3. Change of histological characteristics of ventral prostate; high magnification. (A) Ventral prostate (VP) (x400) for NC mice: mitosis (inset), focal tufting (arrow), thin fibromuscular layer around each duct and loose stroma. (B) VP (×400) for C mice: columnar epithelium and stromal adipose tissue (arrow). (C) VP (×400) for TE mice: focal tufting and papillary formation of the epithelium (arrow). (D) VP (×400) for TBECHαβ mice: cuboidal to proliferative, stratified epithelium. (E) VP (×400) for TBECHγδ mice: tufting with apoptotic bodies (inset) and elongated nuclei. (F) VP (×400) for DPTE mice: cuboidal to low columnar epithelium, without signs of hyperplasia.

significantly lower height in the DLP compared to TE mice (Figs. 3D, 4 D and S2).

In the TBECHγδ-treated mice, features of hyperplasia were identified (Figs. 2E, 3 E and 4 E). The total number of acini in both the VP and DLP and acini diameter in DLP were significantly higher compared to C mice and the epithelium was prominently tufted (Figs. 3E, 4 E and S2). In the VP and DLP, tufting was extended in the peripheral and proximal ducts, and nuclei were focally elongated and slightly hyperchromatic. Apoptotic bodies were frequently encountered (Figs. 3E and 4 E).

Finally, the DPTE-treated mice showed a significant decrease in the number of acini compared to the NC mice in both the VP and DLP (Figs. 2F and S2). The epithelium was cuboidal to low columnar (Figs. 3F

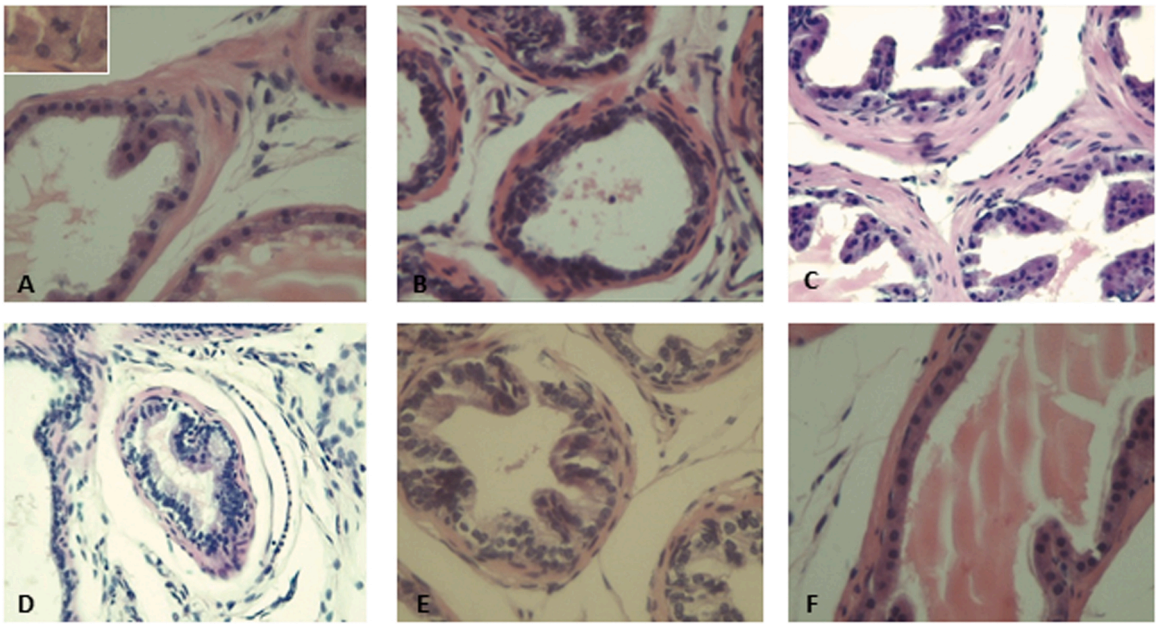

Fig. 4. Change of histological characteristics of dorsolateral prostate; high magnification. (A) Dorsolateral prostate (DLP) (×400) for NC mice: mitosis (inset) and columnar epithelium with moderate epithelial tufting. (B) DLP (×400) for C mice: thin fibromuscular layer and columnar epithelium; minimal tufting and infoldings. (C) DLP (×400) for TE mice: prominent tufting of the epithelium. (D) DLP (×400) for TBECHαβ mice: less tufting than in the NC or TE mice, but more prominent compared to the C mice. (E) DLP (×400) for TBECHγδ mice: increased tufting compared to NC and C mice, similar to that observed in TE mice. (F) DLP (×400) for DPTE mice: cuboidal to low columnar epithelium, minor tufting.

and 4 F) and the mean diameter of acinar lumens was similar to that of the NC mice (Fig. S2).

3.4. Transcriptomic analysis

Microarray analysis was used to identify genes regulated by TE, TBECHαβ, TBECHγδ and DPTE using RNA isolated from mouse prostate. Comparison of gene expression in C compared with NC mice showed that castration altered the expression of 1183 genes among which 586 were upregulated and 597 were downregulated (Fig. 5; Table 2). Treatment of C mice with TE affected higher number of genes than castration alone (695 upregulated and 628 downregulated). Of these NC and TE had 356 common upregulated and 307 common downregulated genes. The remaining genes were either unique to NC or TE. TBECHγδ affected fewer genes than TE (217 upregulated and 248 downregulated). Of these 128 upregulated genes were in common with NC while 163 were in common with TE. Likewise, TBECHγδ had 122 downregulated genes in common with NC and 156 downregulated genes in common with TE. Thus, there was a substantial overlap in gene regulation between NC, TE and TBECHγδ. On the other hand, treatment with TBECHαβ, affected only a few genes (34 upregulated and 27 downregulated). Analysis of gene expression in DPTE treated group demonstrated that only 13 genes were downregulated, and 28 genes were

Table 2
Differentially regulated genes. Number of significantly differentially expressed genes (DEGs) in TBECHαβ, TBECHγδ and TE-injected mice and vehicle-injected non-castrated (NC) mice compared with vehicle-injected C mice.

	NC	TE	TBECHγδ	TBECHαβ
Downregulated genes	597	628	248	27
Upregulated genes	586	695	217	34
Total genes	1183	1323	465	61

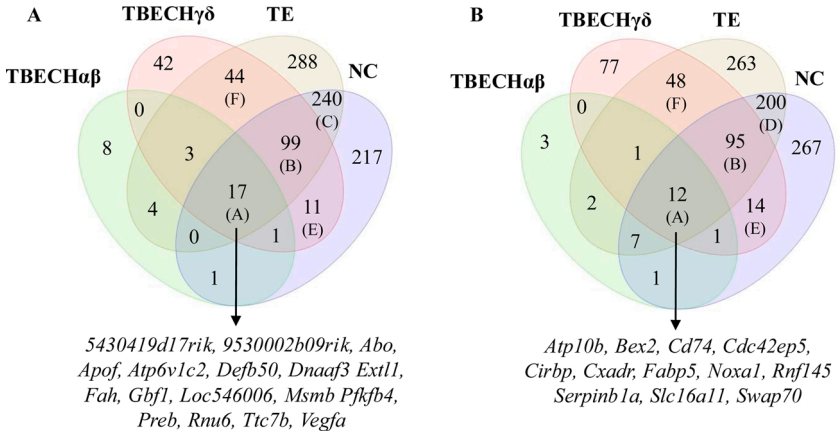

Fig. 5. Venn diagram analysis. Differentially expressed prostate genes in TBECHαβ-, TBECHγδ- and TE-injected castrated (C) and vehicle-injected NC mice as compared to vehicle-injected castrated mice. Comparison of the significantly upregulated genes (A) and the significantly downregulated genes (B). Numbers of genes expressed differentially are shown in the diagrams. The letters in the brackets refer to heatmaps in Fig. S9.

upregulated (Fig. 6; Table 3).

3.5. Validation of microarray data

To verify the transcriptomic data, qRT-PCR analysis was performed with the RNA samples used in the microarray experiments. Nine genes, which were upregulated or downregulated were selected based on substantial changes in expression in the microarray and/or their involvement in significantly overrepresented biological processes. Of these 9 genes, 3 (*beta-microseminoprotein*; *Msmb*, *Apolipoprotein F*; *Apof* and *fatty acid binding protein 5, epidermal*; *Fabp5*) were common for TBECHαβ, TBECHγδ, TE and NC, 4 (*NK3 homeobox 1*; *Nkx3-1*, *FK506 binding protein 5*; *Fkbp5*, *cyclin-dependent kinase inhibitor 1A*; *Cdkn1A* and *Crystallin Mu*; *Crym*) were common for TBECHγδ, TE and NC. One gene, the androgen receptor (*Ar*) was common for TE and NC and 1 (*Insulin like growth factor binding protein 3*; *Igfbp3*) was common for TBECHγδ and TE. Overall, the microarray data and qRT-PCR data were highly consistent with a Pearson correlation of above 0.95 for the compared genes (Fig. S3).

3.6. Pathway analyses of differentially expressed genes and gene ontology

To determine the affected biological processes and gain insights into the functional consequences of castration and the different treatments, GSEA and functional analyses of the DEGs were performed. GSEA indicated that the significantly enriched biological processes for NC compared to C involve, response to stress, localization and transport, including organic substance, vesicle-mediated, nitrogen compound and intracellular transport (Table 4; Fig. S4). Many of the DEGs after TE administration were associated with response to stress, localization, transport, immune system related processes and metabolism (Table 4; Fig. S5). Most of the significantly enriched processes following TBECHγδ treatment were associated with metabolic processes (including positive regulation of protein, small molecule, and cellular modified amino acid metabolic processes), cell cycle associated processes and catabolic processes (Table 4; Fig. S6). TBECHαβ treatment resulted in enrichment of immune system related, cell adhesion, localization and transport processes (Table 4; Fig. S7). Significantly altered genes in response to DPTE were clustered in several processes, particularly regulation processes including negative regulation of nitrogen compound, macromolecule, cellular and protein metabolic processes along with apoptotic signaling pathway processes (Table 4; Fig. S8). The complete list of significantly enriched GO terms of TE, TBECHαβ and TBECHγδ treated C mice compared to vehicle-treated C mice, of vehicle-treated NC mice compared to vehicle-treated C mice and of DPTE-treated NC mice compared to vehicle treated NC mice is available as Supporting information 1.

Further analysis of the GO enrichment data revealed that certain processes were regulated in response to different treatments, including immune system processes (NC, TE, TBECHγδ and TBECHαβ), apoptotic processes and epithelial cell proliferation (NC, TE and TBECHγδ), regulation of lymphocyte proliferation (NC, TE and TBECHαβ), regulation of cell cycle (TE, TBECHγδ and DPTE), steroid biosynthetic processes, steroid metabolic processes and prostate gland epithelium morphogenesis (NC and TE). Notably, several processes involved in prostate gland development, growth and morphogenesis were significantly enriched in response to TE treatment (Table 5).

Table 3
Differentially regulated genes. Number of significantly differentially expressed genes (DEGs) in DPTE-injected mice and vehicle-injected castrated (C) mice compared with vehicle-injected NC mice.

	C	DPTE
Downregulated genes	586	13
Upregulated genes	597	28
Total genes	1183	41

In order to determine the significantly enriched pathways, the DEGs were further analyzed using DAVID Bioinformatics Database. Enriched pathways included TNF and prolactin signaling pathways (NC and TE), NF-kappa B and p53 signaling pathways (TE and TBECHγδ), cell cycle (TE and DPTE), steroid biosynthesis (NC), PCa (TE) and for TBECHγδ, initiation of oocyte maturation by progesterone (Table 6). Although no pathway was affected by all four treatments, there were several DEGs shared between these pathways, particularly DEGs involved in the regulation of the PCa pathway.

3.7. Comparative analysis of DEGs responsive to castration, TE, TBECH and DPTE

We hypothesized that treatment with TE would reverse the expression of genes affected by castration. We also hypothesized that the gene expression profiles of TE and the strong androgen agonist TBECHγδ would be similar while the expression profiles of the androgen antagonist DPTE would be similar to castration. In order to test this, we first compared the regulated genes in response to TBECHαβ, TBECHγδ, TE and NC (Figs. 5; S9). We observed 17 upregulated and 12 downregulated common genes across all four treatments. Comparison of TBECHγδ, a strong androgen agonist, with TE and NC showed that they shared 116 upregulated genes and 107 downregulated genes. Comparison of TE with NC showed that these treatments shared 240 upregulated and 207 downregulated genes. For the complete list of genes see Supporting information 2. Thus, TE treatment reversed the levels of 60 % of the genes downregulated by castration and 53 % of the upregulated genes. This leaves a substantial number of genes that are not related to direct androgen regulation following castration. A large number of these genes were involved in cellular transport functions (Fig. S4). In addition, TBECHγδ showed a similar gene expression pattern with TE resulting in approximately 30 % commonly upregulated and 34 % commonly downregulated genes (Figs. 5; S9). Thus, while TBECHγδ is a potent androgen agonist, it also regulates genes that are not androgen

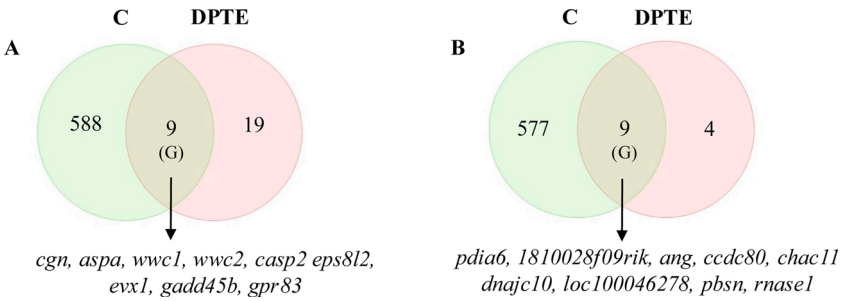

Fig. 6. Venn diagram analysis. Differentially expressed prostate genes in DPTE-injected NC mice and vehicle-injected castrated (C) mice as compared to vehicle-injected NC mice Comparison of the significantly upregulated genes (A) and the significantly downregulated genes (B). Numbers of genes expressed differentially are shown in the diagrams. The letters in the brackets refer to heatmaps in Fig. S9.

Table 4
Top 10 biological processes. Gene ontology (GO) enrichment analysis was performed using Partek Genomic Suite 6.6 and overrepresented biological processes were determined. Ranking of biological processes are shown based on p values in the process. All groups were compared to vehicle-injected castrated mice.

	GO ID	GO Term	DEGs	P value
NC	6810	Transport	250	7.08E-17
	51234	Establishment of localization	252	1.35E-15
	51179	Localization	277	2.24E-15
	34976	Response to endoplasmic reticulum stress	34	6.43E-12
	6888	ER to Golgi vesicle-mediated transport	25	7.12E-12
	71702	Organic substance transport	143	9.87E-11
	16192	Vesicle-mediated transport	92	1.70E-10
	48193	Golgi vesicle transport	34	1.11E-09
	71705	Nitrogen compound transport	120	1.44E-09
	46907	Intracellular transport	93	2.13E-09
TE	6950	Response to stress	219	3.51E-12
	2684	Positive regulation of immune system process	86	3.16E-10
	51716	Cellular response to stimulus	199	4.07E-10
	51179	Localization	287	4.81E-10
	44281	Small molecule metabolic process	138	5.75E-10
	51234	Establishment of localization	258	6.16E-10
	2682	Regulation of immune system process	115	1.49E-09
	6810	Transport	248	2.55E-09
	48518	Positive regulation of biological process	380	3.52E-09
	2252	Immune effector process	52	6.98E-09
TBECHγδ	51247	Positive regulation of protein metabolic process	53	9.79E-06
	44281	Small molecule metabolic process	51	1.46E-05
	6575	Cellular modified amino acid metabolic process	12	2.47E-05
	9894	Regulation of catabolic process	31	2.96E-05
	1901564	Organonitrogen compound metabolic process	108	4.23E-05
	8284	Positive regulation of cell proliferation	35	6.36E-05
	45787	Positive regulation of cell cycle	18	6.50E-05
	60054	Positive regulation of epithelial cell proliferation involved in wound healing	3	8.98E-05
	42176	Regulation of protein catabolic process	18	9.51E-05
	1901987	Regulation of cell cycle phase transition	15	1.25E-04
	2460	Adaptive immune response based on somatic recombination of immune receptors built from immunoglobulin superfamily domains	4	4.15E-05
TBECHαβ	22408	Negative regulation of cell-cell adhesion	5	7.25E-05
	51179	Localization	20	3.76E-04
	6810	Transport	18	4.28E-04
	7162	Negative regulation of cell adhesion	5	4.93E-04
	51234	Establishment of localization	18	6.57E-04
	71621	Granulocyte chemotaxis	3	7.32E-04
	71702	Organic substance transport	12	1.04E-03
	97530	Granulocyte migration	3	1.13E-03
	31058	Positive regulation of histone modification	3	1.32E-03
	51172	Negative regulation of nitrogen compound metabolic process	11	5.04E-04
	10605	Negative regulation of macromolecule metabolic process	11	8.57E-04
	31324	Negative regulation of cellular metabolic process	11	9.19E-04
	51248	Negative regulation of protein metabolic process	7	1.26E-03
DPTE	97190	Apoptotic signaling pathway	4	1.35E-03
	9892	Negative regulation of metabolic process	11	1.91E-03
	32269	Negative regulation of cellular protein metabolic process	6	4.75E-03
	1933	Negative regulation of protein phosphorylation	4	5.02E-03
	48518	Positive regulation of biological process	16	5.97E-03
	1932	Regulation of protein phosphorylation	7	6.45E-03

responsive genes (ARGs) which is in line with TBECH altering other signaling pathways, including those involved in thyroid function [37].

DPTE treated mice had 9 upregulated and 9 downregulated genes in common with castration (Fig. 6). Since the number of DEGs in response to DPTE was small, we also compared the DEGs of DPTE with TBECHαβ, TBECHγδ and TE. We did not observe any common DEGs in these comparisons (data not shown).

3.8. Androgen responsive gene expression patterns in prostate in response to treatments

To identify the androgenic and anti-androgenic activities of TBECH and DPTE, we further compared the regulated genes with ARGs obtained from the androgen responsive gene database [48]. Several differentially expressed ARGs were identified. Seventeen upregulated and 12 downregulated genes were common to all treatments with 3 of the upregulated and 2 of the downregulated genes being ARGs (Supporting information 3). Common to the TBECHγδ, TE and NC treatments were 24 upregulated and 23 downregulated ARGs. Of the 9 upregulated and 9 downregulated genes common to DPTE and C, 5 upregulated and 5 downregulated genes were ARGs (Fig. 7). Ten upregulated and 15 downregulated ARGs were common to both TBECHγδ and TE treatments. Analysis of the fold-change patterns of these ARGs using scatterplot showed a high correlation between the different treatments (Fig. S10). Taken together, the patterns of ARGs expression confirm that TBECHγδ has androgenic activity acting in similar manner to TE and that DPTE displays anti-androgenic activity, having common ARGs with C.

3.9. Identification of genes involved in prostate cancer progression

Analysis of differentially expressed ARGs associated with PCa revealed several genes (Table 7), common to TBECHγδ exposure, TE exposure and NC mice [49–60]. Among the ARGs, *Msmb*, *Defb1* and *Nkx3.1* were highly regulated in these three groups. In addition we

Table 5
Biological processes with potential roles in androgen regulation. Gene ontology (GO) enrichment analysis was performed using Partek Genomic Suite 6.6 and overrepresented biological processes were determined. The number of differentially expressed genes (DEGs) is indicated.

GO ID	GO Term	NC	TE	TBECHγδ	TBECHαβ	DPTE
43066	Regulation of apoptotic process	114	136	43		
50670	Regulation of lymphocyte proliferation	24	24		3	
2376	Immune system process	89	127	36	8	
51726	Regulation of cell cycle		80	29		5
50678	Regulation of epithelial cell proliferation	29	30	16		
6694	Steroid biosynthetic process	12	11			
8202	Steroid metabolic process	21	25			
60740	Prostate gland epithelium morphogenesis	5	5			
33143	Regulation of intracellular steroid hormone receptor signaling pathway	8				
60742	Epithelial cell differentiation involved in prostate gland development		3			
60442	Branching involved in prostate gland morphogenesis		3			
60736	Prostate gland growth		4			
60768	Regulation of epithelial cell proliferation involved in prostate gland development		3			

Table 6
Pathways selected based on their potential roles in androgen regulation. Functional annotation analysis was performed on DAVID Bioinformatics Database. KEGG and BioCarta pathway mapping were used in analysis and overrepresented pathways were determined. The number of differentially expressed genes (DEGs) is indicated.

Pathway	NC	TE	TBECHγδ	DPTE
TNF signaling pathway	12	20		
Prolactin signaling pathway	9	13		
Prostate cancer		12		
Steroid biosynthesis	5			
NF-kappa B signaling pathway		21	7	
Cell cycle		18		3
How progesterone initiates the oocyte maturation			4	

identified two PCa associated genes, namely *Wwc1 and Gadd45b* [61,62], that were common to DPTE exposure and castration (Table 7).

4. Discussion

Androgens regulate a wide range of developmental and physiological processes and are critical for proper differentiation, maturation and maintenance of the prostate gland. Androgen signaling stimulates proliferation and secretory activity and inhibits cell death *via* binding and activating AR [1,2,63]. Disruption of androgen signaling can cause several developmental disturbances of secondary male sexual characteristics, including reduced sperm counts, increased infertility, testicular dysgenesis syndrome, testicular cancer and PCa [64,65]. Understanding how BFRs influence androgen regulation is of a high concern not only for our basic understanding of their possible long-term impact on health but also for developing possible preventative actions.

Using a combination of molecular modeling and *in vitro* bioassays, we have earlier shown that TBECH activates the human AR [26] and regulate ARGs, such as prostate specific antigen (PSA) in LNCaP cells [25]. We have also shown that the androgenic effects of TBECH diastereomers are highly dependent on the amino acid composition of AR ligand binding domain. Thus, AR mutations found in PCa can increase the potency of AR activation [66]. In addition, TBECH shows species specificity in AR responses due to small differences in AR sequence [32–34]. We also discovered DPTE as a potent anti-androgen [32] with similar potency in all so far studied species [32–34].

Analysis of the tissue distribution of compounds following injection with a mixture of equal amounts of 6 BFRs indicated that the bioaccumulation of the compounds was highest in fat followed by prostate and liver. The accumulation of DPTE was higher than the other compounds in all tissues. Previous studies have reported tissue distribution of BFRs, including polybrominated biphenyls (PBBs) and polybrominated diphenyl ethers (PBDEs) [67–69] indicating that these compounds primarily accumulate in fat. Consistent with our data, oral administration of 2.2 mg BDE-99/kg BW resulted in highest accumulation in fat and minor amounts in all other tissues [67]. In another study with rats, oral administration of vinclozolin, a known anti-androgenic compound, resulted in highest accumulation in fat and lowest in testis [70]. Thus, the present results on tissue distribution of the compounds are consistent with earlier studies.

Determination of the BW in response to treatments indicated that the BW increased in TE- and TBECHγδ-treated as compared to vehicle-treated C animals whereas no significant increase was observed compared to vehicle-treated NC animals, suggesting that TE and TBECHγδ prevented castration-induced weight loss. A study with NC rats showed that 28 days exposure to TBECH at 10, 50, 250 and 1250 mg/kg doses through diet had no significant effect on BW whereas a rapid decrease in BW was observed with a 5000 mg/kg dose [37] indicating that the effects of TBECH on BW of NC mice are dose-dependent. In the present study, DPTE exposure did not change the BW compared to the NC animals. This is in contrast to a previous study where decreased BW compared to NC controls was observed for rats orally administrated with the anti-androgenic compounds vinclozolin and dibutyl phthalate [71].

Analysis of changes in prostate size demonstrated that both TBECHγδ and TE exposure increased the PW significantly while DPTE exposure reduced the PW to castration levels. The observed increase in PW by TBECHγδ and TE is in agreement with earlier studies where androgen replacement following castration-induced prostatic involution, induced regrowth and reprogrammed the genome of the prostate in several model animals [2,72–76]. Consistent with the DPTE effect, earlier studies have shown that exposure to anti-androgenic compounds results in prostate involution similar to castration [77,78]. The effects of TBECHγδ and DPTE observed in the present study suggest that exposure to these BFRs may alter the growth pattern of the prostate.

Histopathological analyses are widely used to probe for androgenic and anti-androgenic effects of chemicals. Several previous studies have shown that castration results in prostate atrophy, involving involution of distal segments and changes associated with glandular regression, such as decrease in epithelium folding and acini number and/or diameter; and that androgen replacement returns the gland to its former size and shape by regenerating the lost histological characteristics after castration [77,79–81]. Mouse prostate consists of four lobe pairs, VP, LP, DP (often referred together as dorsolateral prostate, DLP) and AP [82]. Of these, VP has a high sensitivity to androgen ablation and testosterone replacement after castration [83]. Thus, several previous studies have focused on the effects of androgenic/anti-androgenic compounds in the VP [77,84]. In the present study, we observed significant effects of

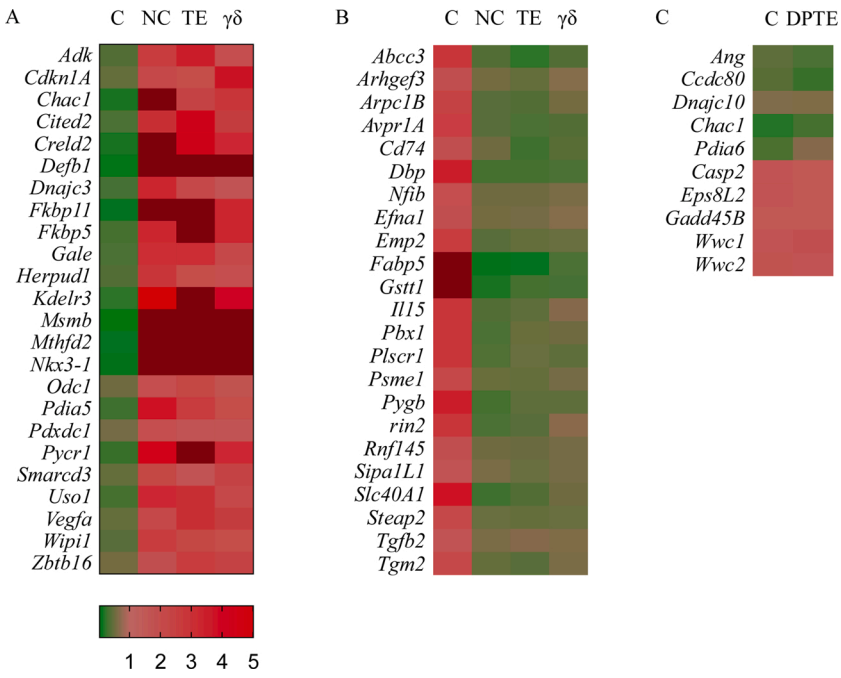

Fig. 7. Heatmaps of differentially expressed androgen-responsive genes. The ARGs list gathered from ARGDB was used as a reference to determine the ARGs affected in the microarray analysis. A) Common upregulated ARGs among vehicle-injected NC and TE- or TBECHγδ-injected C mice. B) Common downregulated ARGs among vehicle-injected NC and TE- or TBECHγδ-injected C mice. C) Common ARGs among vehicle-injected C and DPTE-injected NC mice. GraphPad Prism 7 was used to represent genes as a heatmap.

treatments on VP and DLP. Consistent with previous studies, the VP and DLP of C mice were atrophic and displayed a significant decrease in the number and size of acini compared to NC mice. Besides, the VP and DLP of C mice showed low to tall columnar epithelium with minor tufting, while there were more prominent epithelium tufting and infoldings in the VP and DLP of NC mice. TE treatment reversed the number and size of acini back to almost normal levels in both VP and DLP. These results suggested that studying VP and DLP histological changes constitutes a good experimental approach towards evaluating the androgenic/anti-androgenic effects of TBECH and DPTE. Similar to C group, treatment with DPTE significantly decreased the epithelial tufts, papillae and infoldings as well as the number of acini in VP and DLP. These findings are, therefore, consistent with those of previous studies, in which anti-androgenic compounds such as flutamide, bicalutamide and nilutamide resulted in tissue remodeling towards prostate involution similar to castration [77,78]. On the other hand, and similarly to TE, TBECHγδ treatment resulted in prominent tufting in the epithelium and significantly increased the number of acini in the VP and DLP compared to C mice, while the acini diameter showed an increase only in the DLP. The TBECHαβ group did not show an increase in the number of acini in any lobes but in acini diameter in the DLP with less tufting and infoldings in epithelium compared to NC and TE mice. Considering these current observations and our previous studies, we suggest that, in contrast to DPTE, TBECH could induce prostate regrowth. In particular, TBECHγδ displayed strong TE-like AR agonist activity on the VPs and DLPs of C animals, causing an increase in the number of acini, prominent tufting or papillary formations of the epithelium and even slight cellular atypia. TBECHαβ showed a weaker AR agonist activity compared to TE and TBECHγδ, with less acini and less epithelial tufting. On the other hand, DPTE showed an AR antagonist activity, with a decrease in the number of acini, and epithelium without prominent tufting and papillary projections, when compared to NC and C mice. Taken together, histopathological data suggest that TBECH and DPTE treatments induce prostate regrowth and involution *via* androgenic and anti-androgenic activities, respectively.

As exposure to TBECH and DPTE altered growth and histology of the prostate, we performed microarray analysis on the different exposures to better understand the involvement of androgenic and antiandrogenic pathway regulation in the observed effects. We observed that several of the top enriched processes in response to castration were enriched after TE administration and that treatment with TBECHγδ and TBECHαβ also involved the same GO terms. Comparison of the present data with previous findings [2] on biological processes following castration and androgen supplementation showed that several of the shared processes were involved in androgen regulation. Of these, immune system processes, regulation of apoptotic processes, epithelial cell proliferation, and regulation of lymphocyte proliferation are initiated by castration and repressed following hormone replacement [2,72]. Regulation of cell cycle, steroid biosynthetic processes, steroid metabolic processes and prostate gland epithelium morphogenesis were also significantly enriched GO terms in response to treatment. The observed enrichment of these molecular events is consistent with previous results showing that castration and TE administration alter these processes [2,85].

Similar to GO enrichment analysis, we found that TE reversed the effect of castration at the gene expression level in mouse prostate. Most of the genes that were reprogrammed in response to TE were also affected by TBECHγδ, while TBECHαβ treatment affected a comparatively smaller number of genes. To better understand the androgenic and anti-androgenic activities of TBECH and DPTE, we compared the regulated genes with ARGs from the ARG database [48]. We identified several ARGs shared by the different treatments. The higher number of ARGs regulated by TBECHγδ is in line with our earlier studies [24,25,27] demonstrating that TBECHγδ is a more potent androgenic compound than TBECHαβ.

We further analyzed the roles of the ARGs identified in the present study and identified several well-known PCa related genes. One of these, *Fkbp5,* encodes an immunophilin that influences prostate physiology in the presence of androgens [86]. It has been observed that *Fkbp5* expression is upregulated in LNCaP cells following exposure to androgens, implying that it may have a role in PCa [53]. In another study, the expression of this gene was induced following testosterone replacement after castration [2]. Consistent with these findings, we also observed that TE and TBECHγδ induced *Fkbp5* expression. *Trpv6*, a membrane protein that functions as a calcium channel, is another promising biomarker of tumor progression and has been shown to be strongly expressed in advanced PCa [87]. TBECHγδ significantly upregulated the expression of *Trpv6,* further supporting that TBECH may be involved in tumorigenesis.

Table 7
Androgen responsive genes (ARGs) associated with prostate cancer. Data are fold-changes of gene expression.

Gene ID	C	NC	TE	TBECHγδ	TBECHαβ	DPTE
Msmb	−37.99	37.99	71.01	49.08	19.75	
Defb1	−27.93	27.93	18.51	12.20		
Nkx3-1	−15.18	15.18	11.60	6.67		
Gpx3	−6.89	6.89		5.45		
Pycr1	−4.40	4.40	6.24	3.16		
Fkbp5	−3.23	3.23	5.62	3.34		
Cited2	−2.96	2.96	4.34	2.57		
Herpud1	−2.73	2.73	2.01	1.92		
Wipi1	−2.51	2.51	2.21	2.01		
Trpv6	−2.39	2.39		2.70		
Cdkn1A	−2.18	2.18	2.02	3.68		
Vegfa	−2.15	2.15	2.97	2.56	1.92	
Odc1	−1.90	1.90	2.22	1.74		
Zbtb16	−1.83	1.83	2.61	2.32		
Iqgap2	−1.67	1.67		1.87		
Timp4			11.86	4.28		
Asrgl1			2.32	1.61		
Cyp27A1			2.18	2.20		
Ccnd2			1.89	2.20		
Ccnd3			1.88	1.50		
Stim1			1.86	2.10		
Fabp5	11.80	−11.80	−10.74	−2.94	−2.89	
Gstt1	6.61	−6.61	−3.25	−3.17		
Pygb	3.60	−3.60	−2.26	−2.26		
Dbp	3.54	−3.54	−3.26	−2.91		
Pbx1	2.92	−2.92	−2.12	−1.97		
Il15	2.76	−2.76	−2.32	−1.53		
Abcc3	2.71	−2.71	−5.15	−2.66		
Avpr1A	2.50	−2.50	−3.05	−2.69		
Psme1	2.12	−2.12	−2.17	−1.76		
Steap2	2.07	−2.07	−2.19	−2.09		
Nfib	1.95	−1.95	−1.94	−1.75		
Efna1	1.82	−1.82	−1.84	−1.55		
Tgfb2	1.70	−1.70	−1.52	−1.60		
Wwc1	1.64					1.92
Gadd45b	1.61					1.54
Fbln1			−4.07	−2.86		
Idh1			−2.62	−2.89		
Socs2			−2.55	−2.27		
Inmt			−2.47	−2.39		
Igfbp3			−2.07	−2.30		
Nfkbia			−1.91	−1.56		
Dpp4			−1.91	−1.91		
Dkk3			−1.76	−1.64		
Antxr2			−1.71	−1.51		

We found that TE and TBECHγδ repressed *Steap2* expression and induced *Cdkn1A* expression. This is in agreement with an earlier study showing that repression of *Steap2* resulted in induction of *Cdkn1A* thus leading to cellular apoptosis [88]. It has also been reported that overexpression of *Steap2* induce normal prostate cells to migrate and invade, suggesting that its expression may promote PCa progression [89]. However, the role of *p21/Cdkn1A* in PCa remains unclear as it has also been reported that deletion of *p21/Cdkn1A* results in reduced prostate tumorigenesis [54]. Altogether, the regulation of these genes by TBECHγδ in prostate is particularly important since it has been previously reported that these genes play major roles in the onset of PCa. Based on these findings, TBECHγδ should be considered a high human health concern due to the possible involvement in PCa initiation and/or progression.

Of special interest for PCa was *Msmb*, a PCa biomarker secreted by the epithelial cells of the prostate [49]. While castration significantly downregulated this gene, it was highly upregulated in response to TE, TBECHαβ and TBECHγδ. Consistent with this observation, we previously found that *Msmb* was upregulated by TBECHγδ treatment in several *in vitro* cell based assays [27,66,90]. We have previously observed that *Msmb* is significantly downregulated *in vitro* in the human breast cancer T47-D cell line and the non-transformed prostate RWPE1 cell line and *in vivo* in zebrafish following exposure to DPTE [32,34,90]. However, in the present study, DPTE did not show any effect on *Msmb* expression. This suggests that DPTE-mediated *Msmb* regulation could be context-dependent or that longer exposure time could be required for *in vivo* effects in mice. Interestingly, we identified two PCa associated genes, namely *Wwc1 and Gadd45b* that were common to DPTE exposure and castration (Table 7). It has been previously found that deletion of *Gadd45b* results in suppression of testosterone-induced prostate hyperplasia in mice [62]. In another study, it has also been shown that *Wwc1* is a positive regulator in PCa cell proliferation and motility using LNCaP-C4-2 cell line [61]. *Nkx3-1* is a negative regulator of epithelial cell growth in prostate tissue and downregulation of this gene is associated with prostate tumor progression [50,51]. Castration significantly downregulated *Nkx3-1*, while TE and TBECHγδ treatments upregulated its expression. It has previously been reported that *Nkx3-1* is significantly repressed after castration and induced upon testosterone replacement [2], which is in accordance with our observations.

The effects on prostate physiology caused by TBECH and DPTE in the present study demonstrate that these compounds qualify as endocrine disrupting substances. TBECHγδ shows high similarities to testosterone treatment, increases PW and reverses the action of castration. DPTE, on the other hand, shows higher similarities to castration as the PW is drastically reduced by either intervention. These compounds also alter the transcriptome of mouse prostate, resulting in gene expression patterns highly similar to those observed in PCa. The effects of environmental exposures to pesticides on the development of PCa has been extensively studied, and a significant correlation between exposure and PCa has been identified [91–94]. In a recent study on the risk of developing aggressive PCa, a significant correlation between exposure to the organochloride dimethoate and PCa was established [95]. The results of the present study add the BFRs TBECH and DPTE to the list of compounds that may contribute to PCa development.

5. Conclusions

In the present study, we used an *in vivo* approach to investigate the impact of TBECH and DPTE on prostate growth, histopathology and altered gene expression of the mouse prostate. TBECHγδ displayed substantial androgenic activity and induced growth and histological changes of the prostate, while DPTE displayed anti-androgenic properties that resulted in prostate involution similar to castration. The comparative analysis of ARGs revealed that well-characterized PCa genes are regulated in response to TBECHγδ and DPTE. The present findings demonstrate that TBECH and DPTE are of high human health concern due to their histopathological effects and effects on the expression of genes involved in PCa.

Data availability

The microarray data has been uploaded to ArrayExpress with accession number: E-MTAB-9760.

Conflict of interest

The authors declare no conflict of interest.

Declaration of Competing Interest

The authors report no declarations of interest.

Acknowledgments

The present study was supported by grants from the Knowledge Foundation Sweden, 20150084 and 20180027 (to PEO) and Örebro University. We thank Prof. Efthymia Kitraki, National and Kapodistrian University of Athens, Greece for all her help and advice. Per Liljelind and Maria Hjelt, Chemistry Department, Umeå University are acknowledged

for assistance with the chemical analysis. Nikos Youroukos, Animal Facility Unit, National Hellenic Research Foundation, Athens, Greece is acknowledged for assistance with the animal experiments.

Appendix A. Supplementary data

Supplementary material related to this article can be found, in the online version, at doi:https://doi.org/10.1016/j.reprotox.2021.04.002.

References

[1] P.C. Marker, A.A. Donjacour, R. Dahiya, G.R. Cunha, Hormonal, cellular, and molecular control of prostatic development, Dev. Biol. 253 (2) (2003) 165–174.
[2] X.D. Wang, B.E. Wang, R. Soriano, J. Zha, Z. Zhang, Z. Modrusan, G.R. Cunha, W. Q. Gao, Expression profiling of the mouse prostate after castration and hormone replacement: implication of H-cadherin in prostate tumorigenesis, Differentiation 75 (3) (2007) 219–234.
[3] C.A. Heinlein, C. Chang, Androgen receptor (AR) coregulators: an overview, Endocr. Rev. 23 (2) (2002) 175–200.
[4] S. Ngan, E.A. Stronach, A. Photiou, J. Waxman, S. Ali, L. Buluwela, Microarray coupled to quantitative RT-PCR analysis of androgen-regulated genes in human LNCaP prostate cancer cells, Oncogene 28 (19) (2009) 2051–2063.
[5] E. Fetter, S. Smetanova, L. Baldauf, A. Lidzba, R. Altenburger, A. Schuttler, S. Scholz, Identification and characterization of androgen-responsive genes in zebrafish embryos, Environ. Sci. Technol. 49 (19) (2015) 11789–11798.
[6] M. Alaee, P. Arias, A. Sjodin, A. Bergman, An overview of commercially used brominated flame retardants, their applications, their use patterns in different countries/regions and possible modes of release, Environ. Int. 29 (6) (2003) 683–689.
[7] C.A. de Wit, An overview of brominated flame retardants in the environment, Chemosphere 46 (5) (2002) 583–624.
[8] I. van der Veen, J. de Boer, Phosphorus flame retardants: properties, production, environmental occurrence, toxicity and analysis, Chemosphere 88 (10) (2012) 1119–1153.
[9] L. Chen, K. Yu, C. Huang, L. Yu, B. Zhu, P.K. Lam, J.C. Lam, B. Zhou, Prenatal transfer of polybrominated diphenyl ethers (PBDEs) results in developmental neurotoxicity in zebrafish larvae, Environ. Sci. Technol. 46 (17) (2012) 9727–9734.
[10] J. He, D. Yang, C. Wang, W. Liu, J. Liao, T. Xu, C. Bai, J. Chen, K. Lin, C. Huang, Q. Dong, Chronic zebrafish low dose decabrominated diphenyl ether (BDE-209) exposure affected parental gonad development and locomotion in F1 offspring, Ecotoxicology 20 (8) (2011) 1813–1822.
[11] M. Wahl, R. Guenther, L. Yang, A. Bergman, U. Straehle, S. Strack, C. Weiss, Polybrominated diphenyl ethers and arylhydrocarbon receptor agonists: different toxicity and target gene expression, Toxicol. Lett. 198 (2) (2010) 119–126.
[12] D. Santillo, I. Labounskaia, R. Stringer, P. Johnston, Report on the analysis of industrial wastewaters from the Frutarom VCM/PVC plant, near Haifa, Israel, and adjacent shoreline sediments for organic contaminants, Greenpeace Research Laboratories Technical Note 03/971997, 1997, pp. 1–25.
[13] E. Cequier, A.C. Ionas, A. Covaci, R.M. Marce, G. Becher, C. Thomsen, Occurrence of a broad range of legacy and emerging flame retardants in indoor environments in Norway, Environ. Sci. Technol. 48 (12) (2014) 6827–6835.
[14] S. Newton, U. Sellstrom, C.A. de Wit, Emerging flame retardants, PBDEs, and HBCDDs in indoor and outdoor media in Stockholm, Sweden, Environ. Sci. Technol. 49 (5) (2015) 2912–2920.
[15] F. Tao, M.A. Abdallah, S. Harrad, Emerging and legacy flame retardants in UK Indoor air and dust: evidence for replacement of PBDEs by emerging flame retardants? Environ. Sci. Technol. 50 (23) (2016) 13052–13061.
[16] G. Zheng, Y. Wan, S. Shi, H. Zhao, S. Gao, S. Zhang, L. An, Z. Zhang, Trophodynamics of emerging brominated flame retardants in the aquatic food web of Lake Taihu: relationship with organism metabolism across trophic levels, Environ. Sci. Technol. 52 (8) (2018) 4632–4640.
[17] Y. Ruan, X. Zhang, J.W. Qiu, K.M.Y. Leung, J.C.W. Lam, P.K.S. Lam, Stereoisomer-specific trophodynamics of the chiral brominated flame retardants HBCD and TBECH in a marine food web, with implications for human exposure, Environ. Sci. Technol. 52 (15) (2018) 8183–8193.
[18] Y.F. Ruan, J.C.W. Lam, X.H. Zhang, P.K.S. Lam, Temporal changes and stereoisomeric compositions of 1,2,5,6,9,10-hexabromocyclododecane and 1,2-dibromo-4-(1,2-dibromoethyl)cyclohexane in Marine Mammals from the South China Sea, Environ. Sci. Technol. 52 (5) (2018) 2517–2526.
[19] E. Cechova, M. Seifertova, P. Kukucka, S. Vojta, I. Quaak, M. de Cock, M. van de Bor, A. Kocan, An effective clean-up technique for GC/EI-HRMS determination of developmental neurotoxicants in human breast milk, Anal. Bioanal. Chem. 409 (5) (2017) 1311–1322.
[20] L.C. Guo, S. Yu, Wu, J. Huang, T. Liu, J. Xiao, W. Huang, Y. Gao, X. Li, W. Zeng, S. Rutherford, W. Ma, Y. Zhang, L. Lin, Disruption of thyroid hormone regulated proteins and gene expression by polychlorinated biphenyls, polybrominated diphenyl ethers and new flame retardants in residents of an e-waste region, Environ. Pollut. 254 (Pt B) (2019), 112925.
[21] A. Covaci, S. Harrad, M.A. Abdallah, N. Ali, R.J. Law, D. Herzke, C.A. de Wit, Novel brominated flame retardants: a review of their analysis, environmental fate and behaviour, Environ. Int. 37 (2) (2011) 532–556.
[22] K.H. Nguyen, M. Abou-Elwafa Abdallah, T. Moehring, S. Harrad, Biotransformation of the flame retardant 1,2-dibromo-4-(1,2-dibromoethyl)cyclohexane (TBECH) in vitro by human liver microsomes, Environ. Sci. Technol. 51 (18) (2017) 10511–10518.
[23] G. Arsenault, A. Lough, C. Marvin, A. McAlees, R. McCrindle, G. MacInnis, K. Pleskach, D. Potter, N. Riddell, E. Sverko, S. Tittlemier, G. Tomy, Structure characterization and thermal stabilities of the isomers of the brominated flame retardant 1,2-dibromo-4-(1,2-dibromoethyl)cyclohexane, Chemosphere 72 (8) (2008) 1163–1170.
[24] S. Asnake, A. Pradhan, J. Banjop-Kharlyngdoh, C. Modig, P.E. Olsson, 1,2-Dibromo-4-(1,2 dibromoethyl) cyclohexane (TBECH)-mediated steroid hormone receptor activation and gene regulation in chicken LMH cells, Environ. Toxicol. Chem. 33 (4) (2014) 891–899.
[25] H. Khalaf, A. Larsson, H. Berg, R. McCrindle, G. Arsenault, P.E. Olsson, Diastereomers of the brominated flame retardant 1,2-dibromo-4-(1,2 dibromoethyl)cyclohexane induce androgen receptor activation in the hepg2 hepatocellular carcinoma cell line and the lncap prostate cancer cell line, Environ. Health Perspect. 117 (12) (2009) 1853–1859.
[26] A. Larsson, L.A. Eriksson, P.L. Andersson, P. Ivarson, P.E. Olsson, Identification of the brominated flame retardant 1,2-dibromo-4-(1,2-dibromoethyl)cyclohexane as an androgen agonist, J. Med. Chem. 49 (25) (2006) 7366–7372.
[27] A. Pradhan, J.B. Kharlyngdoh, S. Asnake, P.E. Olsson, The brominated flame retardant TBECH activates the zebrafish (Danio rerio) androgen receptor, alters gene transcription and causes developmental disturbances, Aquat. Toxicol. 142-143 (2013) 63–72.
[28] L.C. Raiford, D.J. Birosel, The action of bromine on certain mixed ethers, J. Am. Chem. Soc. 51 (6) (1929) 1776–1778.
[29] W. Vetter, R. Recke, P. Ostrowicz, N. Rosenfelder, Liquid chromatographic enantioseparation of the brominated flame retardant 2,3-dibromopropyl-2,4,6-tribromophenyl ether (DPTE) and enantiomer fractions in seal blubber, Chemosphere 78 (2) (2010) 134–138.
[30] J. Sauer, E. Antusch, C. Ripp, Monitoring of lipophilic organic pollutants in sewer systems by sewer slime analysis, Vom Wasser 88 (1997) 49–69.
[31] M. Shoeib, T. Harner, G.M. Webster, E. Sverko, Y. Cheng, Legacy and current-use flame retardants in house dust from Vancouver, Canada, Environ. Poll. (Barking, Essex : 1987) 169 (2012) 175–182.
[32] J.B. Kharlyngdoh, A. Pradhan, S. Asnake, A. Walstad, P. Ivarsson, P.E. Olsson, Identification of a group of brominated flame retardants as novel androgen receptor antagonists and potential neuronal and endocrine disrupters, Environ. Int. 74 (2015) 60–70.
[33] S. Asnake, A. Pradhan, J.B. Kharlyngdoh, C. Modig, P.E. Olsson, The brominated flame retardants TBP-AE and TBP-DBPE antagonize the chicken androgen receptor and act as potential endocrine disrupters in chicken LMH cells, Toxicol. In Vitro 29 (8) (2015) 1993–2000.
[34] A. Pradhan, S. Asnake, J.B. Kharlyngdoh, C. Modig, P.E. Olsson, In silico and biological analysis of anti-androgen activity of the brominated flame retardants ATE, BATE and DPTE in zebrafish, Chem. Biol. Interact. 233 (2015) 35–45.
[35] B.J. Park, V. Palace, K. Wautier, B. Gemmill, G. Tomy, Thyroid axis disruption in juvenile brown trout (Salmo trutta) exposed to the flame retardant beta-tetrabromoethylcyclohexane (beta-TBECH) via the diet, Environ. Sci. Technol. 45 (18) (2011) 7923–7927.
[36] S.C. Marteinson, V. Palace, R.J. Letcher, K.J. Fernie, Disruption of thyroxine and sex hormones by 1,2-dibromo-4-(1,2-dibromoethyl)cyclohexane (DBE-DBCH) in American kestrels (Falco sparverius) and associations with reproductive and behavioral changes, Environ. Res. 154 (2017) 389–397.
[37] I.H. Curran, V. Liston, A. Nunnikhoven, D. Caldwell, M.J. Scuby, P. Pantazopoulos, D.F. Rawn, L. Coady, C. Armstrong, D.E. Lefebvre, G.S. Bondy, Toxicologic effects of 28-day dietary exposure to the flame retardant 1,2-dibromo-4-(1,2-dibromoethyl)-cyclohexane (TBECH) in F344 rats, Toxicology 377 (2017) 1–13.
[38] S.C. Marteinson, R.J. Letcher, L. Graham, S. Kimmins, G. Tomy, V.P. Palace, I. J. Ritchie, L.T. Gauthier, D.M. Bird, K.J. Fernie, The flame retardant beta-1,2-dibromo-4-(1,2-dibromoethyl)cyclohexane: fate, fertility, and reproductive success in American kestrels (Falco sparverius), Environ. Sci. Technol. 46 (15) (2012) 8440–8447.
[39] P.Y. Liu, T. Meng, Y.Y. Li, M. Cai, X.H. Li, J. Chen, Z.F. Qin, Tetrabromoethylcyclohexane affects gonadal differentiation and development in the frog Pelophylax nigromaculatus, Aquat. Toxicol. 192 (2017) 40–47.
[40] W. Vetter, C. Gallistl, A. Schlienz, T. Preston, J. Muller, K.T. von der Trenck, Brominated flame retardants (BFRs) in eggs from birds of prey from Southern Germany, 2014, Environ. Pollut. 231 (Pt 1) (2017) 569–577.
[41] T. Chen, M. Huang, J. Li, J. Li, Z. Shi, Polybrominated diphenyl ethers and novel brominated flame retardants in human milk from the general population in Beijing, China: occurrence, temporal trends, nursing infants' exposure and risk assessment, Sci. Total Environ. 689 (2019) 278–286.
[42] Y. Liu, S. Cui, Y. Ma, Q. Jiang, X. Zhao, Q. Cheng, L. Guo, H. Jia, L. Lin, Brominated flame retardants (BFRs) in marine food webs from Bohai Sea, China, Sci. Total Environ. 772 (2021), 145036.
[43] K. Jian, L.M. Zhao, M.L. Ya, Y.Y. Zhang, H.J. Su, W.K. Meng, J.H. Li, G.Y. Su, Dietary intake of legacy and emerging halogenated flame retardants using food market basket estimations in Nanjing, eastern China, Environ. Pollut. 258 (2020).
[44] G.S. Prins, Endocrine disruptors and prostate cancer risk, Endocr. Relat. Cancer 15 (3) (2008) 649–656.
[45] G. Griffin, J.M. Clark, J. Zurlo, M. Ritskes-Hoitinga, Scientific uses of animals: harm-benefit analysis and complementary approaches to implementing the three Rs, Rev. Sci. Tech. 33 (1) (2014) 265–272.

[46] C. Lee, J.A. Sensibar, S.M. Dudek, R.A. Hiipakka, S.T. Liao, Prostatic ductal system in rats: regional variation in morphological and functional activities, Biol. Reprod. 43 (6) (1990) 1079–1086.
[47] D.E. Terry, A.F. Clark, Influence of testosterone on chondroitin sulphate proteoglycan in the rat prostate, Biochem. Cell Biol. 74 (5) (1996) 645–651.
[48] M. Jiang, Y. Ma, C. Chen, X. Fu, S. Yang, X. Li, G. Yu, Y. Mao, Y. Xie, Y. Li, Androgen-responsive gene database: integrated knowledge on androgen-responsive genes, Mol. Endocrinol. (Baltimore, Md.) 23 (11) (2009) 1927–1933.
[49] H. Sakai, T. Tsurusaki, S. Kanda, T. Koji, J.W. Xuan, Y. Saito, Prognostic significance of beta-microseminoprotein mRNA expression in prostate cancer, Prostate 38 (4) (1999) 278–284.
[50] R. Bhatia-Gaur, A.A. Donjacour, P.J. Sciavolino, M. Kim, N. Desai, P. Young, C. R. Norton, T. Gridley, R.D. Cardiff, G.R. Cunha, C. Abate-Shen, M.M. Shen, Roles for Nkx3.1 in prostate development and cancer, Genes Dev. 13 (8) (1999) 966–977.
[51] B. Gurel, T.Z. Ali, E.A. Montgomery, S. Begum, J. Hicks, M. Goggins, C.G. Eberhart, D.P. Clark, C.J. Bieberich, J.I. Epstein, A.M. De Marzo, NKX3.1 as a marker of prostatic origin in metastatic tumors, Am. J. Surg. Pathol. 34 (8) (2010) 1097–1105.
[52] S.S. Forootan, Z.Z. Bao, F.S. Forootan, L. Kamalian, Y. Zhang, A. Bee, C.S. Foster, Y. Ke, Atelocollagen-delivered siRNA targeting the FABP5 gene as an experimental therapy for prostate cancer in mouse xenografts, Int. J. Oncol. 36 (1) (2010) 69–76.
[53] A.M. Velasco, K.A. Gillis, Y. Li, E.L. Brown, T.M. Sadler, M. Achilleos, L. M. Greenberger, P. Frost, W. Bai, Y. Zhang, Identification and validation of novel androgen-regulated genes in prostate cancer, Endocrinology 145 (8) (2004) 3913–3924.
[54] A.K. Jain, K. Raina, R. Agarwal, Deletion of p21/Cdkn1a confers protective effect against prostate tumorigenesis in transgenic adenocarcinoma of the mouse prostate model, Cell Cycle (Georgetown, Tex.) 12 (10) (2013) 1598–1604.
[55] L. Latonen, E. Afyounian, A. Jylha, J. Nattinen, U. Aapola, M. Annala, K. K. Kivinummi, T.T.L. Tammela, R.W. Beuerman, H. Uusitalo, M. Nykter, T. Visakorpi, Integrative proteomics in prostate cancer uncovers robustness against genomic and transcriptomic aberrations during disease progression, Nat. Commun. 9 (1) (2018) 1176.
[56] J. Hoefer, J. Kern, P. Ofer, I.E. Eder, G. Schafer, D. Dietrich, G. Kristiansen, S. Geley, J. Rainer, E. Gunsilius, H. Klocker, Z. Culig, M. Puhr, SOCS2 correlates with malignancy and exerts growth-promoting effects in prostate cancer, Endocr. Relat. Cancer 21 (2) (2014) 175–187.
[57] U.R. Chandran, C. Ma, R. Dhir, M. Bisceglia, M. Lyons-Weiler, W. Liang, G. Michalopoulos, M. Becich, F.A. Monzon, Gene expression profiles of prostate cancer reveal involvement of multiple molecular pathways in the metastatic process, BMC Cancer 7 (2007) 64.
[58] S.H. Shin, G.Y. Lee, M. Lee, J. Kang, H.W. Shin, Y.S. Chun, J.W. Park, Aberrant expression of CITED2 promotes prostate cancer metastasis by activating the nucleolin-AKT pathway, Nat. Commun. 9 (1) (2018) 4113.
[59] Y. Chen, Q. Zhang, Q. Wang, J. Li, C. Sipeky, J. Xia, P. Gao, Y. Hu, H. Zhang, X. Yang, H. Chen, Y. Jiang, Y. Yang, Z. Yao, Y. Chen, Y. Gao, A. Tan, M. Liao, J. Schleutker, J. Xu, Y. Sun, G.H. Wei, Z. Mo, Genetic association analysis of the RTK/ERK pathway with aggressive prostate cancer highlights the potential role of CCND2 in disease progression, Sci. Rep. 7 (1) (2017) 4538.
[60] M. Seifert, C. Peitzsch, I. Gorodetska, C. Borner, B. Klink, A. Dubrovska, Network-based analysis of prostate cancer cell lines reveals novel marker gene candidates associated with radioresistance and patient relapse, PLoS Comput. Biol. 15 (11) (2019), e1007460.
[61] S. Stauffer, X. Chen, L. Zhang, Y. Chen, J. Dong, KIBRA promotes prostate cancer cell proliferation and motility, FEBS J. 283 (10) (2016) 1800–1811.
[62] S.-R. Park, D.-Y. Jung, T.-W. Kim, C.-H. Lee, J.-Y. Jung, Growth arrest and DNA-damage-inducible 45 beta (GADD45β) deletion suppresses testosterone-induced prostate hyperplasia in mice, Life Sci. 211 (2018) 74–80.
[63] N. Kyprianou, J.T. Isaacs, Activation of programmed cell death in the rat ventral prostate after castration, Endocrinology 122 (2) (1988) 552–562.
[64] G. Bagchi, Y. Zhang, K.A. Stanley, D.J. Waxman, Complex modulation of androgen responsive gene expression by methoxyacetic acid, Reprod. Biol. Endocrinol. 9 (2011) 42.
[65] D.C. Luccio-Camelo, G.S. Prins, Disruption of androgen receptor signaling in males by environmental chemicals, J. Steroid Biochem. Mol. Biol. 127 (1-2) (2011) 74–82.
[66] J.B. Kharlyngdoh, S. Asnake, A. Pradhan, P.E. Olsson, TBECH, 1,2-dibromo-4-(1,2 dibromoethyl) cyclohexane, alters androgen receptor regulation in response to mutations associated with prostate cancer, Toxicol. Appl. Pharmacol. 307 (2016) 91–101.
[67] H. Hakk, G. Larsen, E. Klasson-Wehler, Tissue disposition, excretion and metabolism of 2,2',4,4',5-pentabromodiphenyl ether (BDE-99) in the male Sprague-Dawley rat, Xenobiotica 32 (5) (2002) 369–382.
[68] H.B. Matthews, S. Kato, N.M. Morales, D.B. Tuey, Distribution and excretion of 2,4,5,2',4',5'-hexabromobiphenyl, the major component of Firemaster BP-6, J. Toxicol. Environ. Health 3 (3) (1977) 599–605.
[69] J.N. Miceli, B.H. Marks, Tissue distribution and elimination kinetics of polybrominated biphenyls (PBB) from rat tissue, Toxicol. Lett. 9 (4) (1981) 315–320.
[70] A. Sierra-Santoyo, G. Castaneda-Hernandez, R.A. Harrison, H.A. Barton, M. F. Hughes, Pharmacokinetics and dosimetry of the antiandrogen vinclozolin after oral administration in the rat, Toxicol. Sci. 106 (1) (2008) 55–63.
[71] J. Ashby, P.A. Lefevre, The peripubertal male rat assay as an alternative to the Hershberger castrated male rat assay for the detection of anti-androgens, oestrogens and metabolic modulators, J. Appl. Toxicol. 20 (1) (2000) 35–47.
[72] K.V. Desai, A.M. Michalowska, P. Kondaiah, J.M. Ward, J.H. Shih, J.E. Green, Gene expression profiling identifies a unique androgen-mediated inflammatory/immune signature and a PTEN (phosphatase and tensin homolog deleted on chromosome 10)-mediated apoptotic response specific to the rat ventral prostate, Mol. Endocrinol. (Baltimore, Md.) 18 (12) (2004) 2895–2907.
[73] F. Jiang, Z. Wang, Identification of androgen-responsive genes in the rat ventral prostate by complementary deoxyribonucleic acid subtraction and microarray, Endocrinology 144 (4) (2003) 1257–1265.
[74] M. Otto-Duessel, M. He, J.O. Jones, Tissue-selective regulation of androgen-responsive genes, Endocr. Res. 37 (4) (2012) 203–215.
[75] R. Pfundt, F. Smit, C. Jansen, T. Aalders, H. Straatman, W. van der Vliet, J. Isaacs, A.G. van Kessel, J. Schalken, Identification of androgen-responsive genes that are alternatively regulated in androgen-dependent and androgen-independent rat prostate tumors, Genes Chromosomes Cancer 43 (3) (2005) 273–283.
[76] Z. Wang, R. Tufts, R. Haleem, X. Cai, Genes regulated by androgen in the rat ventral prostate, Proc. Natl. Acad. Sci. U. S. A. 94 (24) (1997) 12999–13004.
[77] R.M. Goes, C. Zanetoni, T.C. Tomiosso, D.L. Ribeiro, S.R. Taboga, Surgical and chemical castration induce differential histological response in prostate lobes of Mongolian gerbil, Micron (Oxford, England : 1993) 38 (3) (2007) 231–236.
[78] G.J. Kolvenbag, B.J. Furr, G.R. Blackledge, Receptor affinity and potency of non-steroidal antiandrogens: translation of preclinical findings into clinical activity, Prostate Cancer Prostatic Dis. 1 (6) (1998) 307–314.
[79] B. Felix-Patricio, A.F. Miranda, J.L. Medeiros Jr., C.B.M. Gallo, B.M. Gregorio, D. B. Souza, W.S. Costa, F.J.B. Sampaio, The prostate after castration and hormone replacement in a rat model: structural and ultrastructural analysis, Int. Braz. J Urol. 43 (5) (2017) 957–965.
[80] C.L. Lai, R. van den Ham, G. van Leenders, J. van der Lugt, E. Teske, Comparative characterization of the canine normal prostate in intact and castrated animals, Prostate 68 (5) (2008) 498–507.
[81] Y. Sugimura, G.R. Cunha, A.A. Donjacour, Morphological and histological study of castration-induced degeneration and androgen-induced regeneration in the mouse prostate, Biol. Rreprod. 34 (5) (1986) 973–983.
[82] A. Zingiryan, N.H. Farina, K.H. Finstad, J.L. Stein, J.B. Lian, G.S. Stein, Dissection of individual prostate lobes in mouse models of prostate Cancer to obtain high quality RNA, J. Cell. Physiol. 232 (1) (2017) 14–18.
[83] P.P. Banerjee, S. Banerjee, T.R. Brown, B.R. Zirkin, Androgen action in prostate function and disease, Am. J. Clin. Exp. Urol. 6 (2) (2018) 62–77.
[84] T. Suzuki, N. Fujimoto, S. Kitamura, S. Ohta, Effects of environmental antiandrogenic chemicals on expression of androgen-responsive genes in rat prostate lobes, J. Health Sci. 53 (4) (2007) 401–405.
[85] N. Kyprianou, E.M. Bruckheimer, Y. Guo, Cell proliferation and apoptosis in prostate cancer: significance in disease progression and therapy, Histol. Histopathol. 15 (4) (2000) 1211–1223.
[86] J.A. Magee, L.W. Chang, G.D. Stormo, J. Milbrandt, Direct, androgen receptor-mediated regulation of the FKBP5 gene via a distal enhancer element, Endocrinology 147 (1) (2006) 590–598.
[87] T. Fixemer, U. Wissenbach, V. Flockerzi, H. Bonkhoff, Expression of the Ca2+-selective cation channel TRPV6 in human prostate cancer: a novel prognostic marker for tumor progression, Oncogene 22 (49) (2003) 7858–7861.
[88] L. Wang, Y. Jin, Y.J. Arnoldussen, I. Jonson, S. Qu, G.M. Maelandsmo, A. Kristian, B. Risberg, H. Waehre, H.E. Danielsen, F. Saatcioglu, STAMP1 is both a proliferative and an antiapoptotic factor in prostate cancer, Cancer Res. 70 (14) (2010) 5818–5828.
[89] H. Whiteland, S. Spencer-Harty, C. Morgan, H. Kynaston, D.H. Thomas, P. Bose, N. Fenn, P. Lewis, S. Jenkins, S.H. Doak, A role for STEAP2 in prostate cancer progression, Clin. Exp. Metastasis 31 (8) (2014) 909–920.
[90] J.B. Kharlyngdoh, A. Pradhan, P.E. Olsson, Androgen receptor modulation following combination exposure to brominated flame-retardants, Sci. Rep. 8 (1) (2018) 4843.
[91] M.C.R. Alavanja, C. Samanic, M. Dosemeci, J. Lubin, R. Tarone, C.F. Lynch, C. Knott, K. Thomas, J.A. Hoppin, J. Barker, J. Coble, D.P. Sandler, A. Blair, Use of agricultural pesticides and prostate cancer risk in the agricultural health study cohort, Am. J. Epidemiol. 157 (9) (2003) 800–814.
[92] D.G. Bostwick, H.B. Burke, D. Djakiew, S. Euling, S.M. Ho, J. Landolph, H. Morrison, B. Sonawane, T. Shifflett, D.J. Waters, B. Timms, Human prostate cancer risk factors, Cancer 101 (Suppl. 10) (2004) 2371–2490.
[93] P.A. Cowin, P. Foster, J. Pedersen, S. Hedwards, S.J. McPherson, G.P. Risbridger, Early-onset endocrine disruptor-induced prostatitis in the rat, Environ. Health Perspect. 116 (7) (2008) 923–929.
[94] H. Sun, M.L. Sun, D.B. Barr, Exposure to organophosphorus insecticides and increased risks of health and cancer in US women, Environ. Toxicol. Pharmacol. (2020), 103474.
[95] L.A. Pardo, L.B.E. Freeman, C.C. Lerro, G. Andreotti, J.N. Hofmann, C.G. Parks, D. P. Sandler, J.H. Lubin, A. Blair, S. Koutros, Pesticide exposure and risk of aggressive prostate cancer among private pesticide applicators, Environ. Health-Glob. 19 (1) (2020).